# QED at Critical Field Strength (SLAC Experiment 144)

K.T. McDonald

*Princeton U.*

February 19, 1993

*Are You Lonely ?*

*Work on Your Own ?*

*Hate Having to Make Decisions ?*

# THEN HOLD A MEETING

You can get to See Other People,
Sleep in Peace, Offload Decisions,
Feel Important and Impress
(or BORE)
Your Colleagues

*And All in Work Time*

# MEETINGS,

# THE PRACTICAL

# ALTERNATIVE TO WORK

"Nor is anything empty. For what is empty is nothing. What is nothing cannot be."

–Melissos
Admiral of Samnian navy,
defeated Pericles 441 B.C.

## The QED Critical Field Strength

- O. Klein (Z. Phys. **53**, 157 (1929)) noted that the reflection coefficient is infinite when Dirac electrons hit a steep barrier (Klein's paradox).

- F. Sauter (Z. Phys. **69**, 742 (1931)) deduced that the paradox arises only in electric fields exceeding the critical strength:

$$E_{\text{crit}} = \frac{m^2c^3}{e\hbar} = 1.32 \times 10^{16} \text{ Volts/cm}.$$

- At the critical field, the voltage drop across a Compton wavelength is the electron rest energy:

$$eE_{\text{crit}} \cdot \frac{\hbar}{mc} = mc^2.$$

- At the critical field the vacuum 'sparks' into $e^+e^-$ pairs (Heisenberg and Euler, Z. Phys. **98**, 718 (1936)).

## Where to Find Critical Fields

- The magnetic field at the surface of a neutron star approaches the critical field $B_{\text{crit}} = 4.4 \times 10^{13}$ Gauss.

- During heavy-ion collisions where $Z_{\text{total}} = 2Z > 1/\alpha$, the critical field can be exceeded and $e^+e^-$ production is expected.

  The line spectrum observed in positron production in heavy-ion collisions (Darmstadt) is not understood.

- The electric field of a bunch at a future linear collider approaches the critical field in the frame of the oncoming bunch.

## Critical Fields in $e$-Laser Collisions

- The electric field due to a laser as seen in the rest frame of a high-energy electron is

$$E^\star = \gamma(1+\beta)E_{\rm lab} \approx 2\gamma E_{\rm lab}$$

- The critical field is achieved with a laser beam of intensity

$$I = \frac{E_{\rm lab}^2}{377\Omega} = \frac{E_{\rm crit}^2}{4\gamma^2 \cdot 377}.$$

Thus for 46-GeV electrons ($\gamma = 9 \times 10^4$) we can achieve $E_{\rm crit}$ with a focused laser intensity of $1.43\times 10^{19}$ Watts/cm$^2$

($\Rightarrow \gtrsim 10^{27}$ photons/cm$^3$, $E_{\rm lab} = 7\times 10^{10}$ Volts/cm).

- Such intensities are now attainable in table-top teraWatt (T$^3$) lasers in which a Joule of energy is compressed into one picosecond and focused into a few square microns.

# $\Upsilon$

$$\Upsilon = \frac{E^\star}{E_{\text{crit}}} = \frac{\sqrt{(p_0 E + p \times B)^2 - (p \cdot E)^2}}{m E_{\text{crit}}} = \frac{|p_\mu F^{\mu\nu}|}{m E_{\text{crit}}},$$

where $p_\mu = (p_0, p)$ = 4-vector of probe particle.

$$\Upsilon = \gamma B / E_{\text{crit}} \qquad \text{(constant magnetic field).}$$

In a constant crossed field where $E = B$ and $E \perp B$,

$$\Upsilon = 2\gamma E / E_{\text{crit}} \qquad \text{(linear collider).}$$

For a plane wave with 4-vector $\omega_0 = (\omega_0, k_0)$,

$$\Upsilon = 2\gamma E / E_{\text{crit}} = \eta \frac{(p \cdot \omega_0)}{m^2} \qquad \text{(plane wave field),}$$

where

$$\eta = \frac{eE}{m\omega_0 c} = \frac{e\,|A_\mu|}{mc^2}.$$

For infrared laser light, $\omega_0 = 1.17$ eV,

$$\Upsilon = 0.42\eta \qquad (\lambda_0 = 1.06\ \mu\text{m},\ p_0 = 47\ \text{GeV}).$$

# E-144 Physics Program

1. Nonlinear Compton Scattering: $e + n\omega \rightarrow e' + \gamma'$

   - Semiclassical theory $\Rightarrow$ data will diagnose laser intensity.
   - Provides $\gamma$ beam for light-by-light scattering.

2. Beamstrahlung

   - $E \approx 10^{11}$ V/cm in bunches at future $e^+e^-$ colliders.
   - $e + n\omega_{\text{laser}}$ laser interactions with large $n$ mimic beamstrahlung.
   - $e + n\omega \rightarrow e'e^+e^-$ is analog of important pair-production backgrounds in future colliders.

3. The Multiphoton Breit-Wheeler Reaction:

   $\gamma + n\omega \rightarrow e^+e^-$

   - Might show anomalous structure in $e^+e^-$ invariant mass when $E > E_{\text{crit}}$.

4. Copious $e^+e^-$ Production

- $e^+e^-$ pairs from $e$-laser collisions could be best low-emittance source of positrons.
- No Coulomb scattering in laser 'target.'
- Positrons largely preserve the geometric emittance of the electron beam $\Rightarrow$ 'cooling' of invariant emittance.
- Can produce 1 positron per electron if $\Upsilon > 1$
- Production with visible laser is optimal for $\sim$ 500 GeV electrons.

  [Or use a 50-nm FEL with 50-GeV electrons.]

5. $e$-laser technolgy of E-144 is precursor of $e$-$\gamma$ and $\gamma$-$\gamma$ colliders.

# BEAMSTRAHLUNG EXPERIMENTS

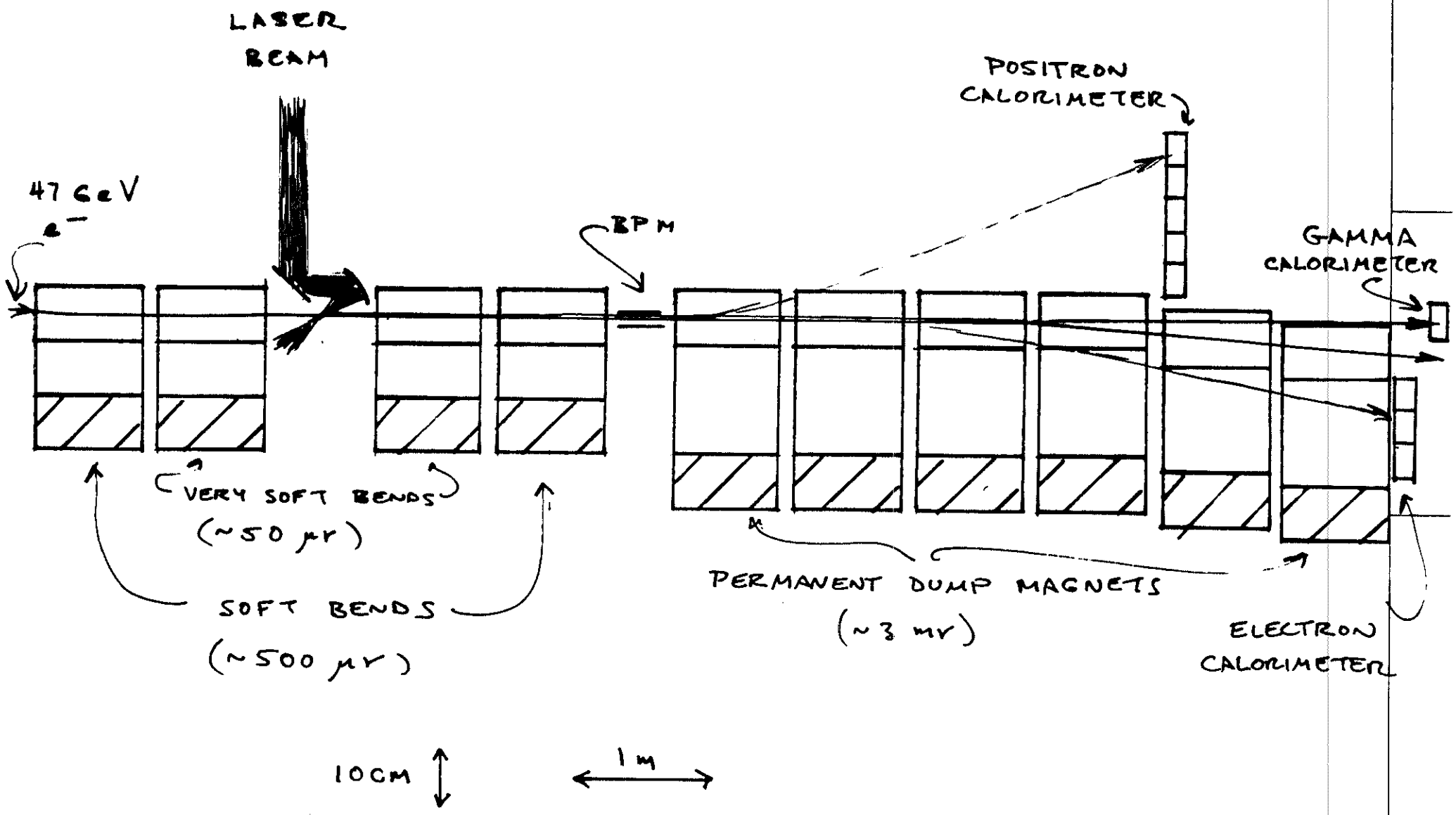

# STRONG-FIELD QED EXPERIMENTS

① NONLINEAR COMPTON SCATTERING

$$e + n\,\omega_{LASER} \rightarrow e' + \gamma$$

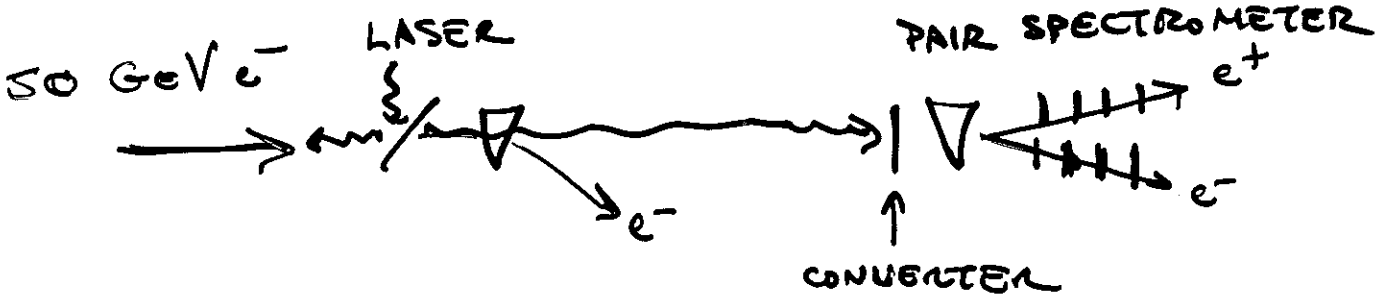


② PAIR CREATION BY LIGHT

$$\gamma + n\,\omega_{LASER} \rightarrow e^+ e^-$$

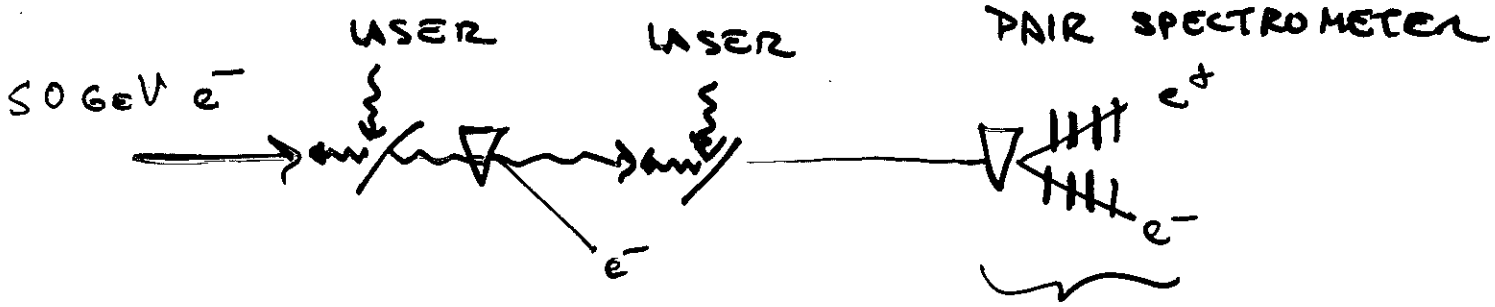


10 keV RESOLUTION

ON $M_{e^+e^-}$ AT 1.8 MeV/$c^2$

## Responsibilities

- $e$-beam ..... SLAC

  $e$-beam diagnostics

  RF timing

  Laser & spectrometer buildings

- Laser systems ..... Rochester

  Laser-beam transport and diagnostics (with SLAC)

- Silicon calorimeters ($e^+$, $e^-$, $\gamma$) ..... Tennessee

  Calorimeter readout (with Princeton)

- CCD Pair Spectrometer ..... Princeton

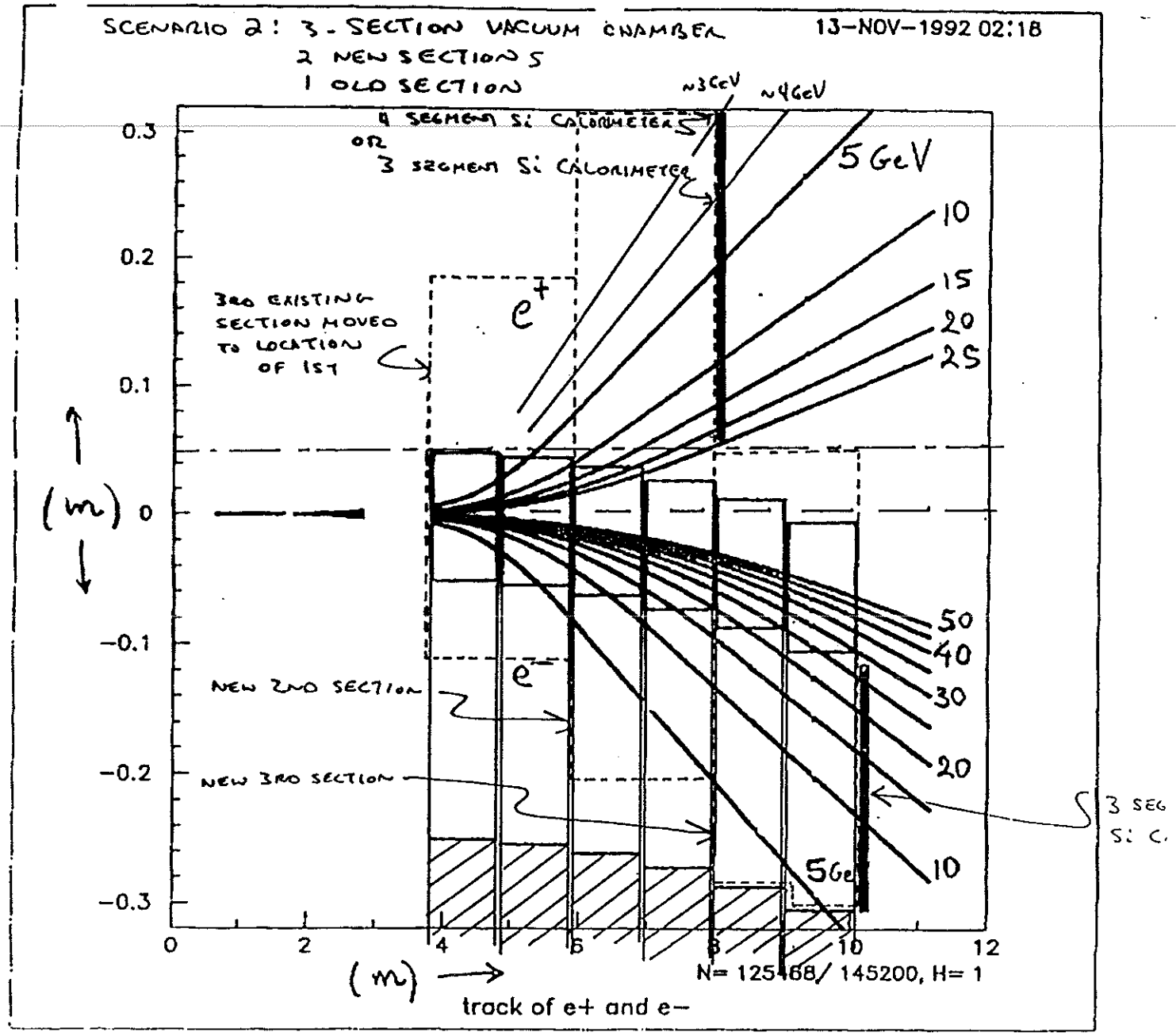


Figure 7: Side view of the layout of the eight dump magnets, showing the proposed location of a 4-module silicon calorimeter for positrons, and a three-module calorimeter for scattered electrons.

# 3 Electron Calorimeter

The configuration of the dump-magnet string is favorable for measurement of scattere electrons of energies between 6 and 30 GeV, supposing the upper limit is set by a requireme that any detector remain 5 cm below the primary beam (see Fig. 7). A silicon calorimet consisting of three modules of U. Tennessee wafers would fit well just downstream of tl sixth dump magnet in the short free space upstream of the $\gamma$-laser interaction point.

The physics interest in such a calorimeter is twofold.

## 3.1 Nonlinear Compton Scattering

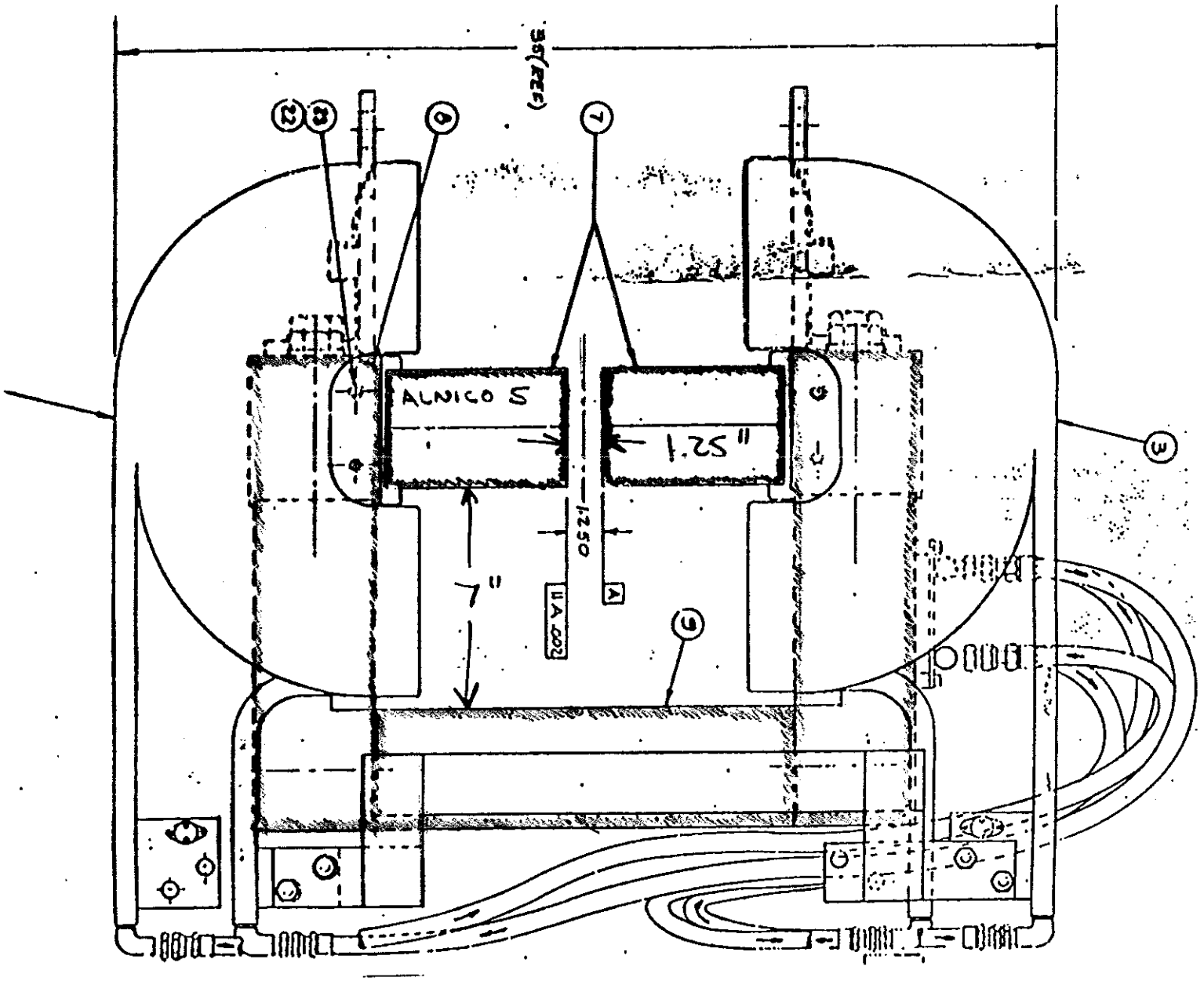


Figure 1: End view of the permanent C-magnets. The gap is 1.25″ wide, the pole tips are 4″ high, and the distance from the bottom of the pole tips to the top of the yoke is 8″. The coils labelled 3 are used only to excite the permanent magnets initially, and are off during normal use. The horizontal gap between the coils is 12″.

itron separately. In this note we are primarily concerned with the positron only, as the astrahlung experiment will not detect coincidences between the electron and positron. Recall that if $p$ is the 4-vector of a positron (or electron) in the field-free region, its ector $\overline{p}$ inside a plane-wave field of strength $\eta \equiv e\boldsymbol{E}/m\omega_0 c$ can be written

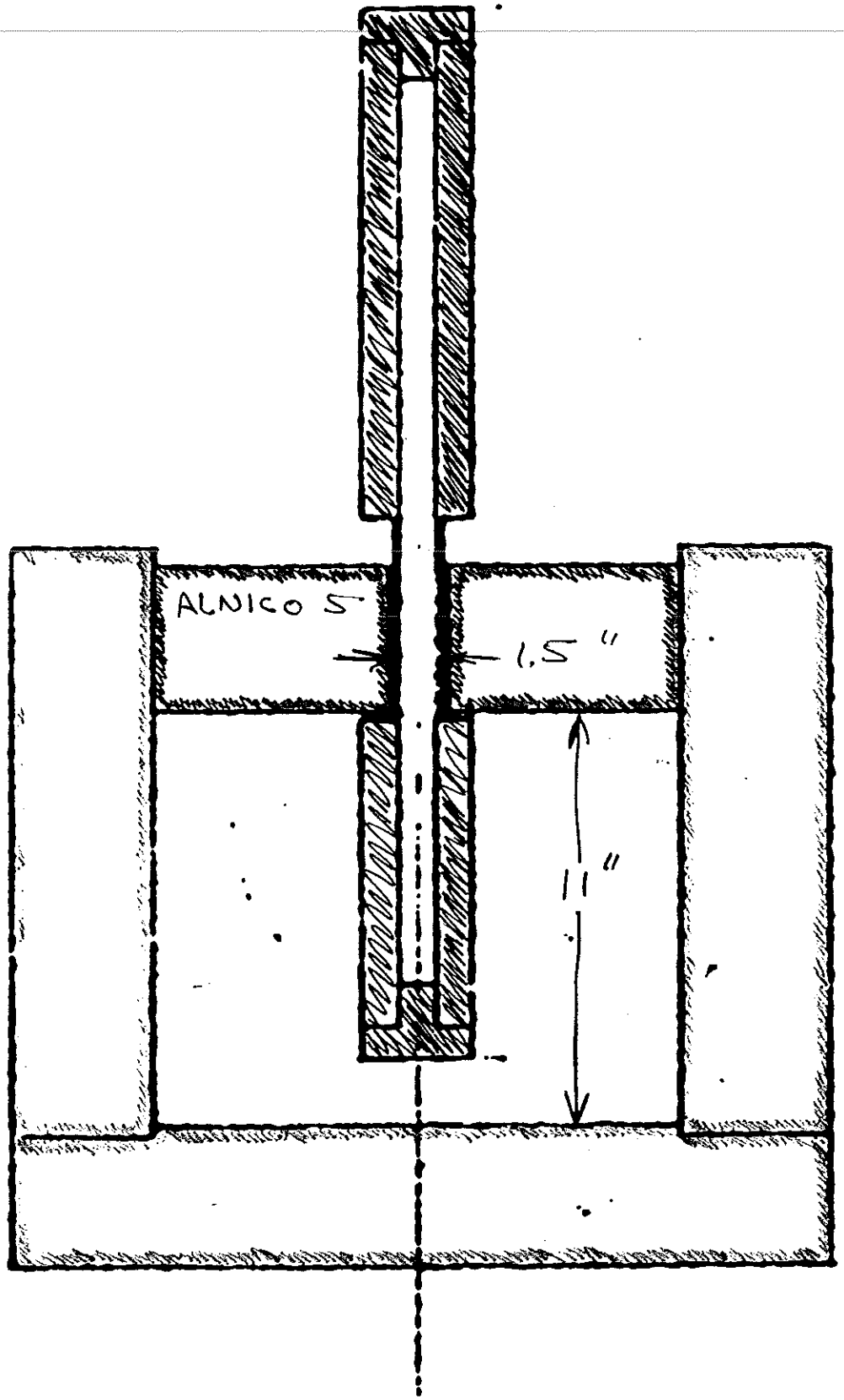


SECT. A-A SCALE 1:8

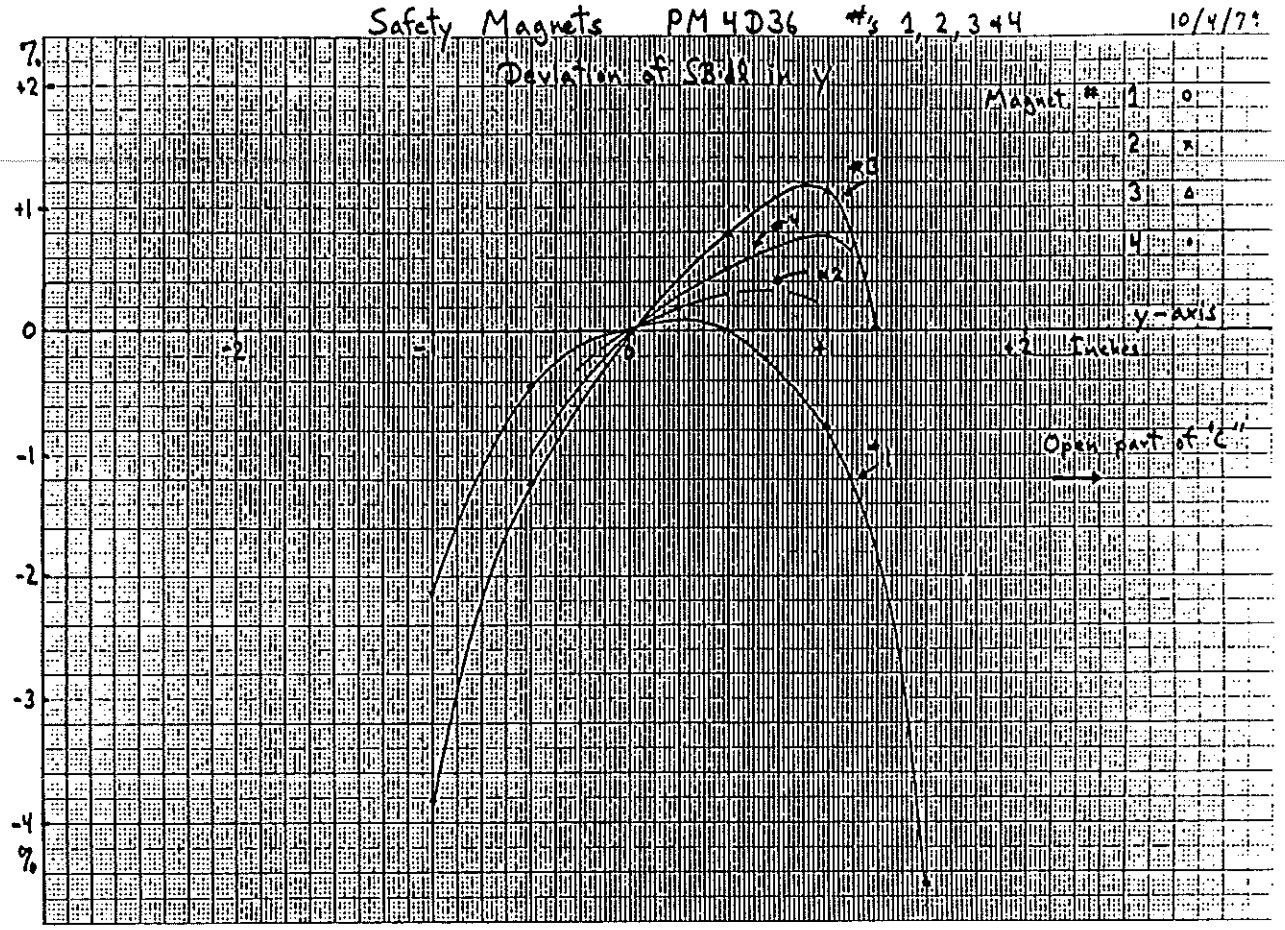


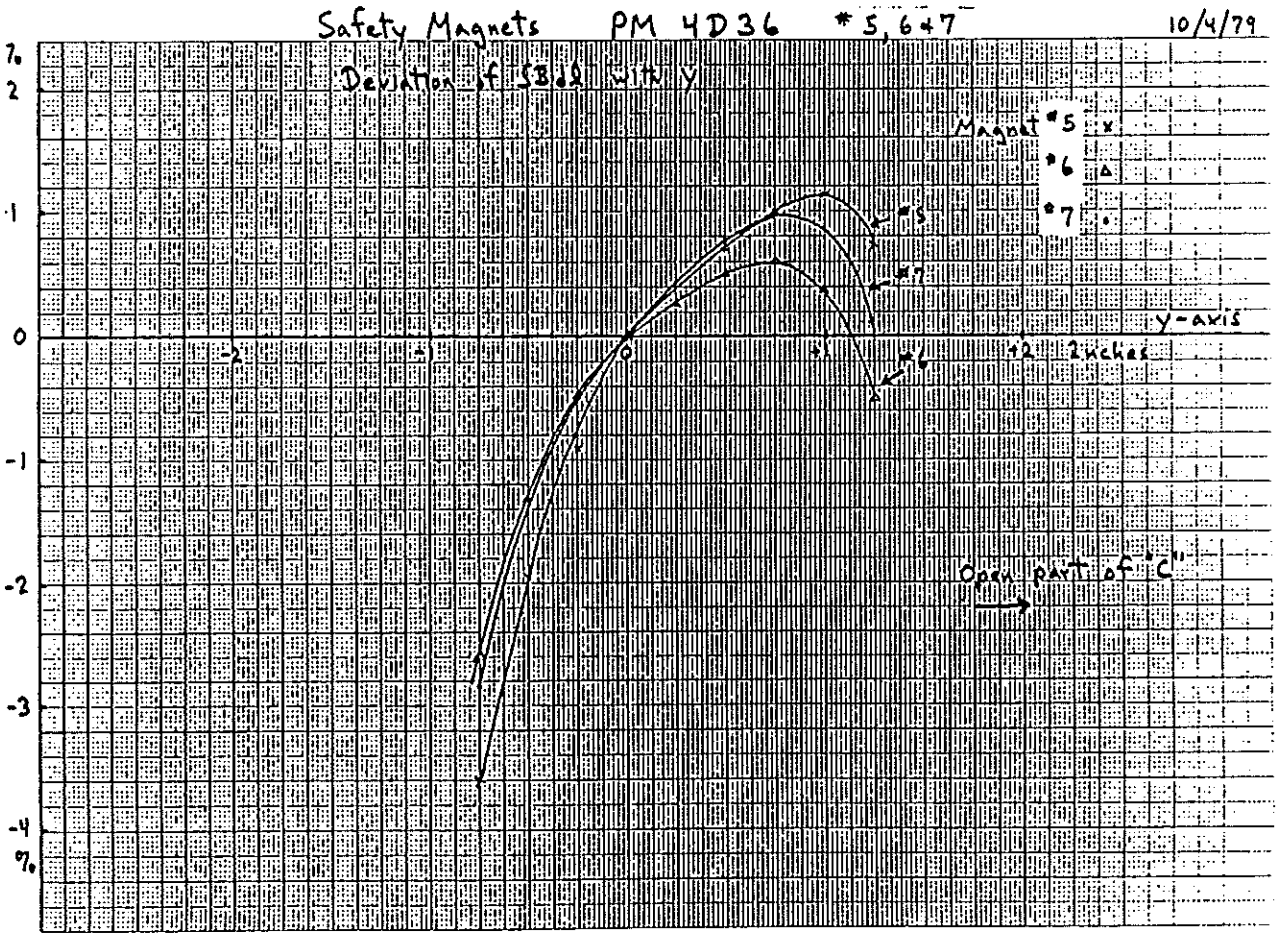


Figure 3: Maps of the variation with height of the field strength in the midplane of the permanents magnets (only 6 of which are available for E-144).

The peak values $B_x(0,0)/B_{\text{gap}}$ are 0.872 and 0.845 for the cases $a = 0.625''$ and $a = 0.75''$, respectively, supposing $b = 2''$ and $T = 6''$. Figure 4 gives plots of $B_x(0,y)/B_x(0,0)$ for the two gaps. The predicted falloff of the field with $y$ is slightly faster than that reported in the magnet maps of 10/4/79.

In both cases we find

$$\int_0^\infty dy B_x(x,y) = 2'' \cdot B_{\text{gap}}$$

to good accuracy. This implies that the $P_t$ kick for particles leaving the top or bottom of the dump magnets will be essentially unchanged when the gap is widened, even though the kick of particles leaving the ends of the magnets is reduced.

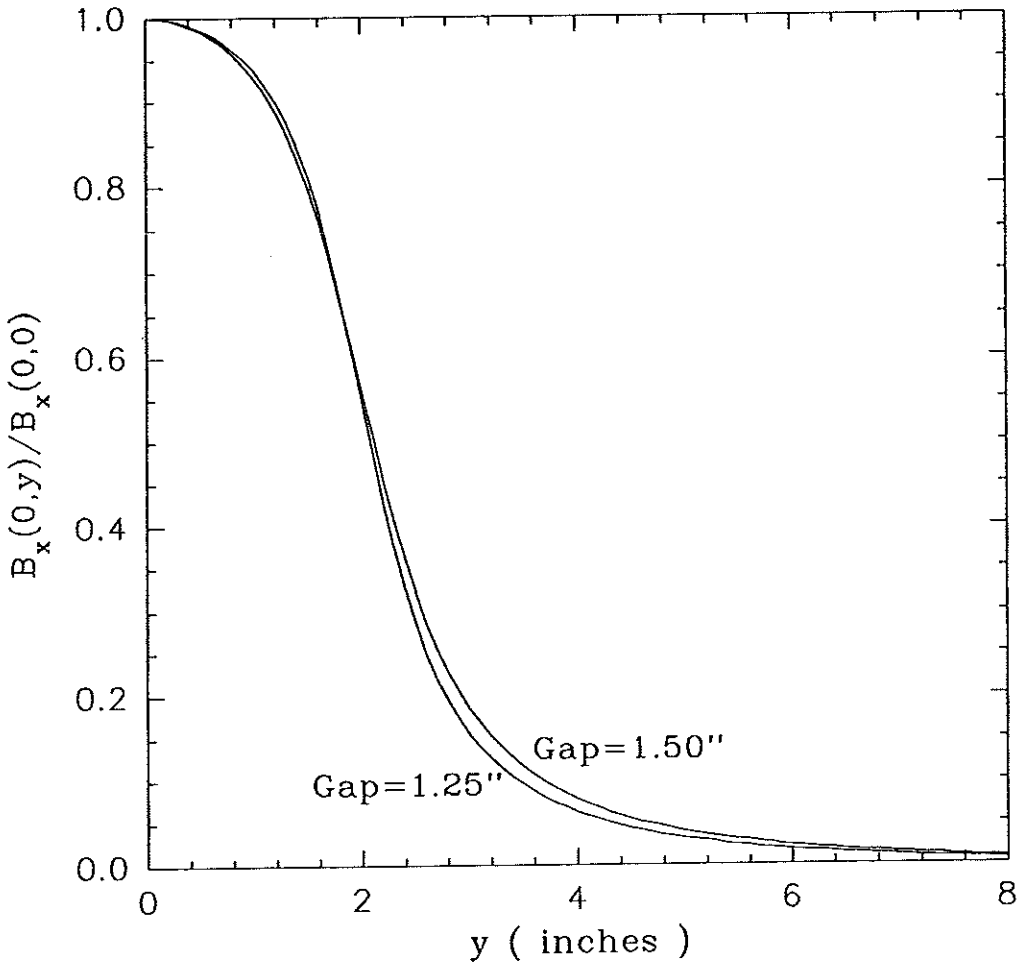


Figure 4: Normalized field profiles calculated for the midplane of the dump magnets for two gap widths.

2/15/93

$\tau_{LASER} = 1\,ps$

$f/D = 5$ $\quad \tau_e = 3\,ps$ $\quad \sigma_{r,e} = 1000\,\mu m$

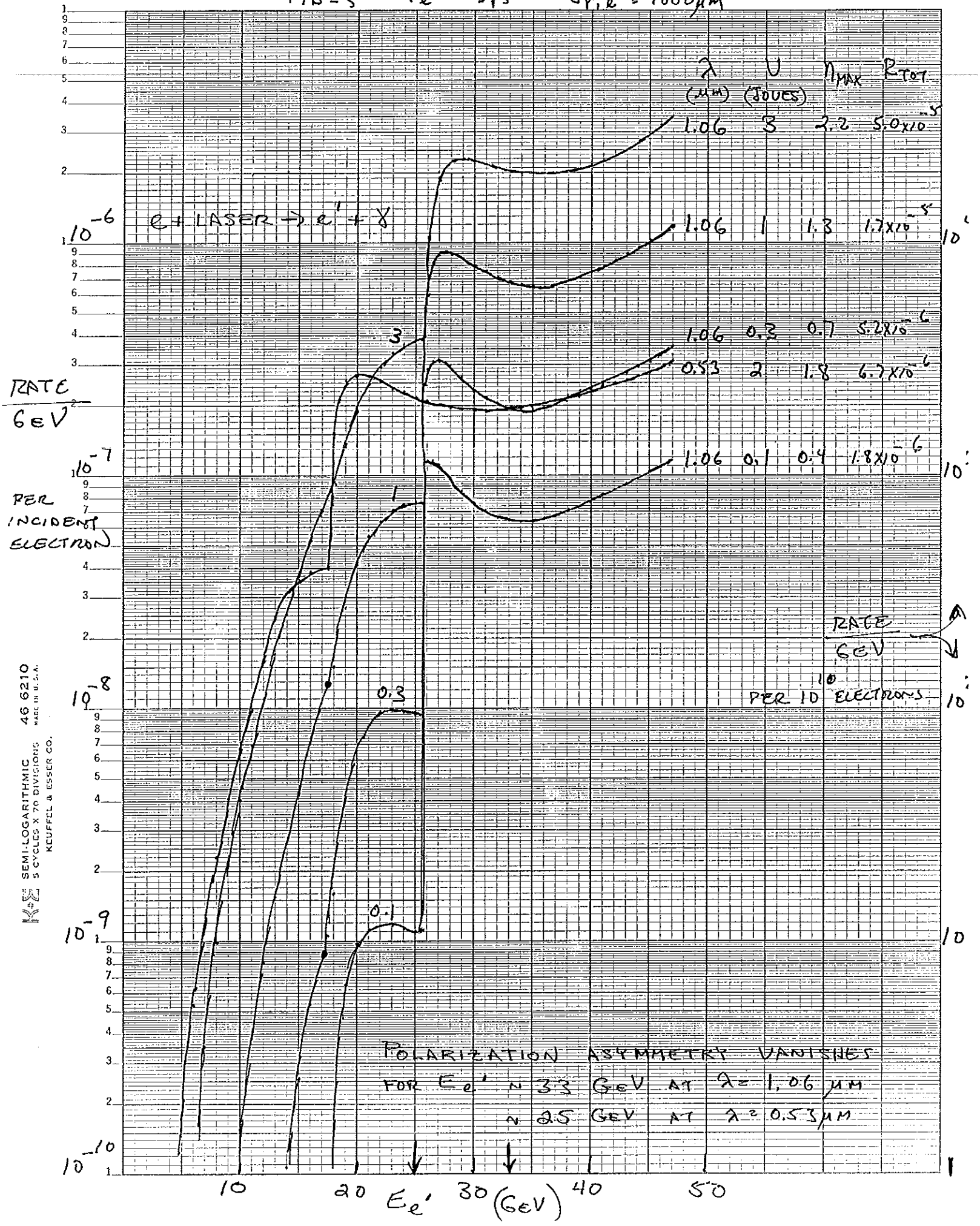

2/4/93 $\lambda = 1.06\,\mu m$ $\eta = 2.2$ $\tau_{LASER} = 1\,ps$ $\sigma_{\gamma,LASER} = 2.4\,\mu m$ $\gamma = 1.0$ AT $E = 50\,GeV$

$U = 3$ JOULES $f/D = 5$ $\tau_e = 3\,ps$ $\sigma_{\gamma,e} = 1000\,\mu m$

MODEL DATE

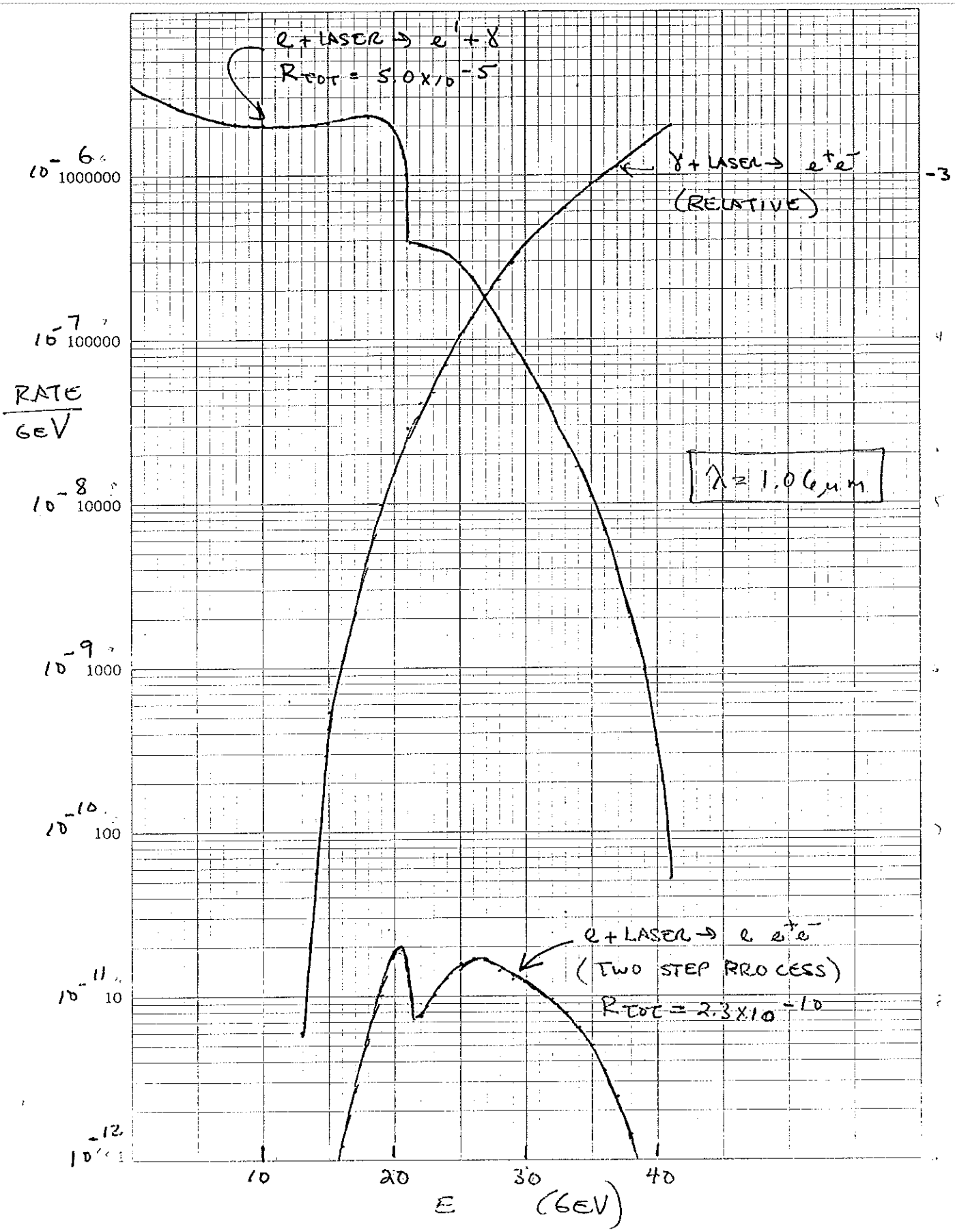


46 6463

SEMI-LOGARITHMIC 7 CYCLES X 60 DIVISIONS KEUFFEL & ESSER CO. MADE IN U.S.A.

$\lambda = 0.53\,\mu m$ $\eta = 1.8$ $\tau_{LASER} = 1\,ps$ $\sigma_{r,LASER} = 1.6\,\mu m$ $\gamma = 1.6$ at $E = 50$ GeV

$U = 2$ Joules $f/D = 5$ $\tau_e = 3\,ps$ $\sigma_{r,e} = 1000\,\mu m$

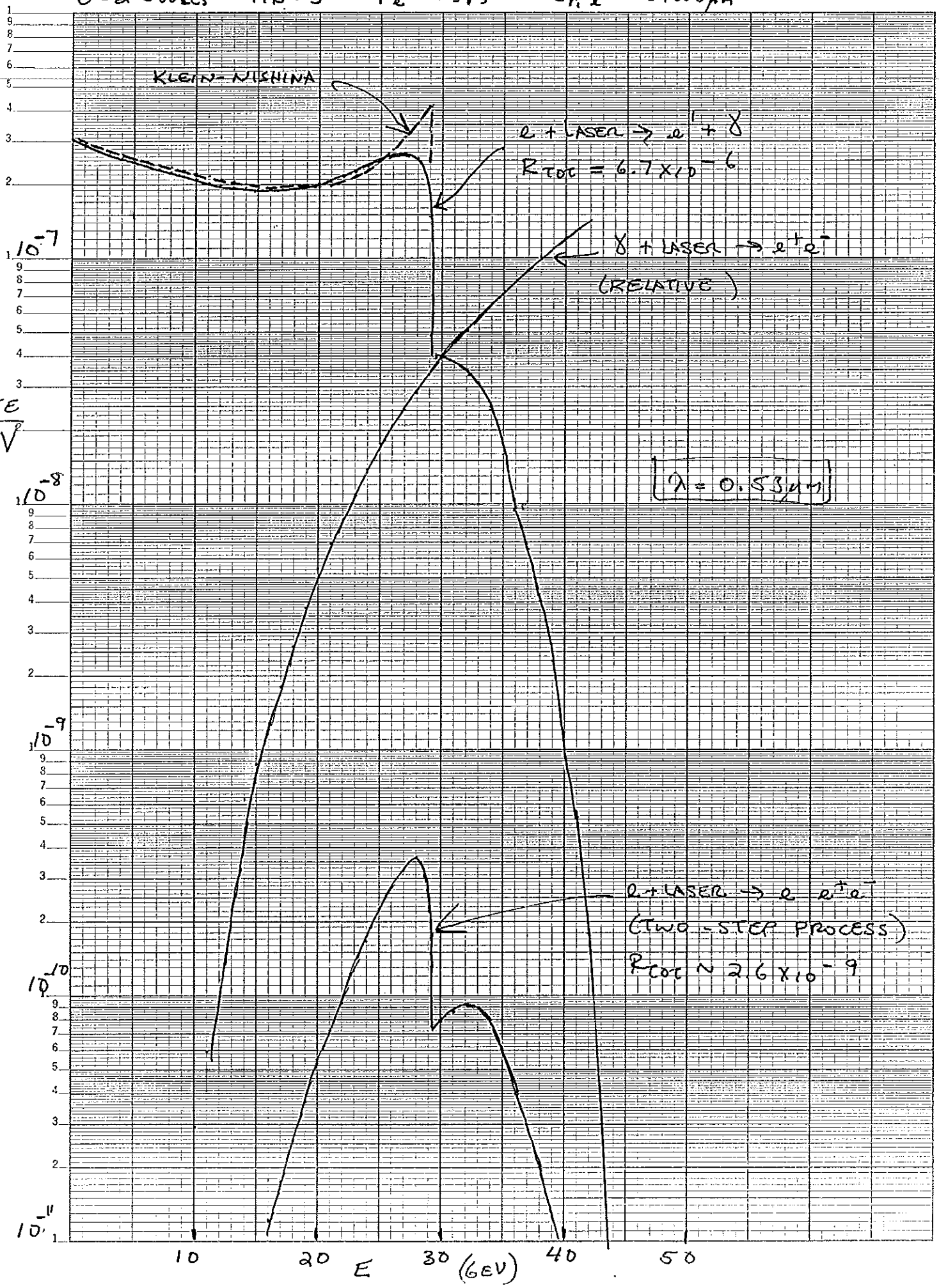

$\lambda = 1.06\,\mu m$ $\quad$ $\eta = 2.2$ $\quad$ $\tau_{LASER} = 1\,ps$ $\quad$ $\sigma_{Y,LASER} = 2.4\,\mu m$ $\quad$ $\Upsilon = 0.5$ AT $E_\gamma = 25$ GeV

$U = 3$ Joules $\quad$ $f/D = 5$ $\quad$ $\tau_\gamma = 3\,ps$ $\quad$ $\sigma_{Y,\gamma} = 3.0\,\mu m$

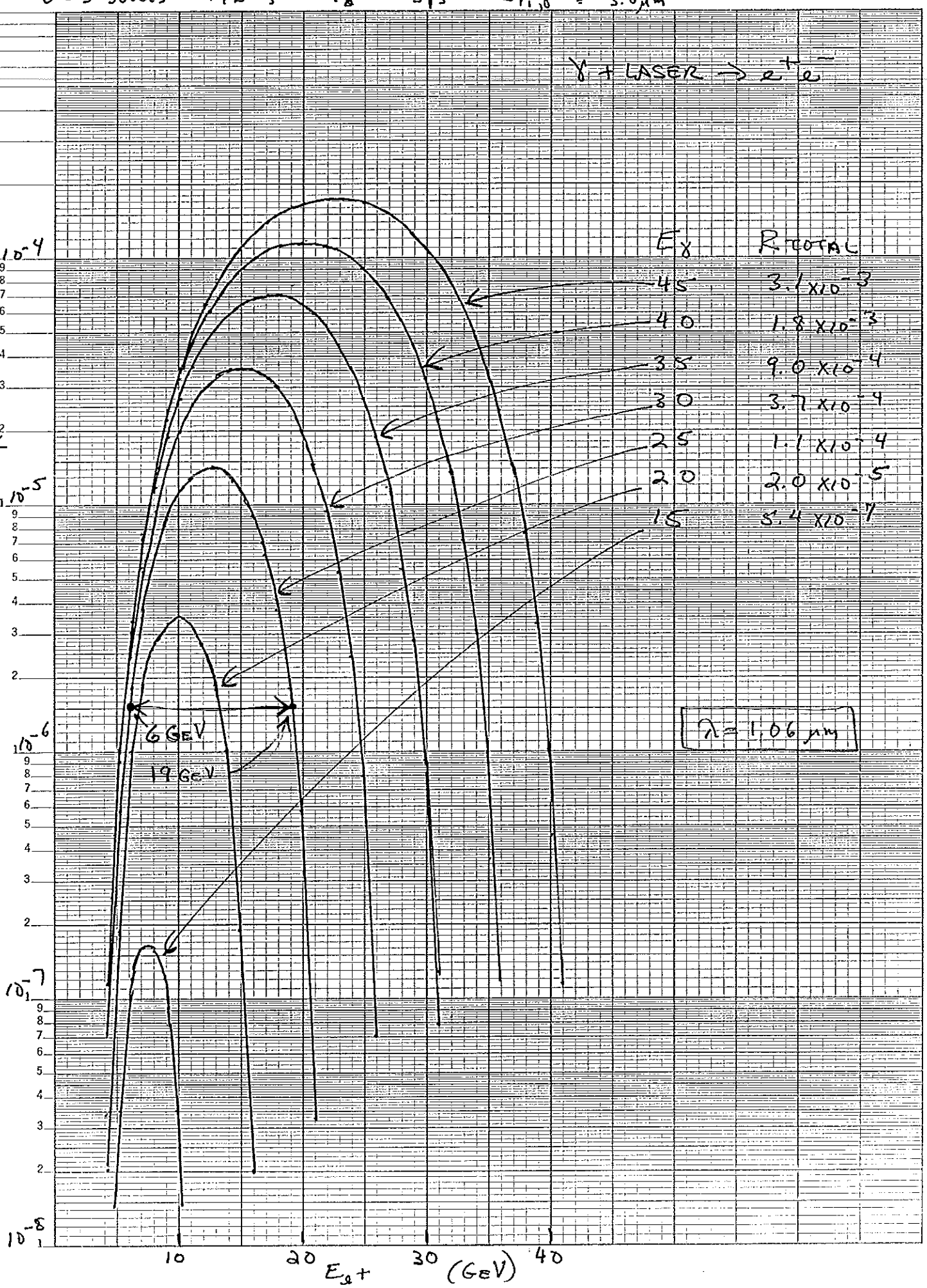

$\lambda = 0.53\,\mu m$ $\quad \eta = 21.0$ $\quad \tau_{LASER} = 1\,ps$ $\quad \sigma_{Y\,LASER} = 1.2\,\mu m$

$U = 2$ JOULES $\quad f/D = 5$ $\quad \tau_{\gamma} = 3\,ps$ $\quad \sigma_{r,\gamma} = 1.5\,\mu m$ $\quad \Upsilon = 0.8$ AT $E_{\gamma} = 25\,GeV$

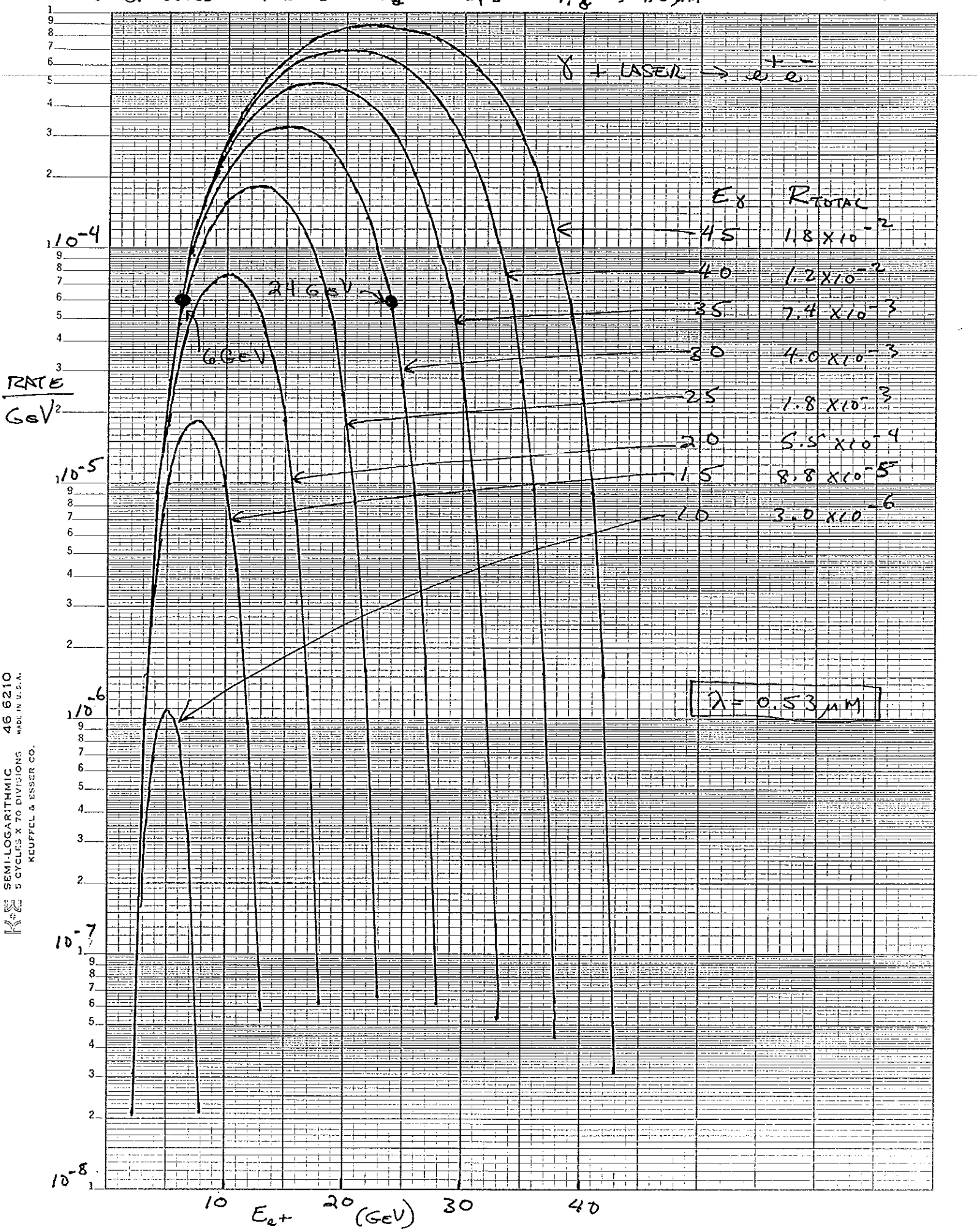

BEAMSTRAHLUNG EXPERIMENTS:

- DEMONSTRATE ABILITY OF FFTB & $T^3$ LASER TO EXPLORE STRONG-FIELD QED.
- MEASURE PROMINENT FEATURES OF NONLINEAR COMPTON SCATTERING & POSITRON PRODUCTION.

PAIR-SPECTROMETER EXPERIMENTS:

- MORE PRECISE CONFRONTATION WITH THEORETICAL UNDERSTANDING OF PHYSICS BEYOND THE QED CRITICAL FIELD STRENGTH.

- THE DEVIL IS IN THE DETAILS....

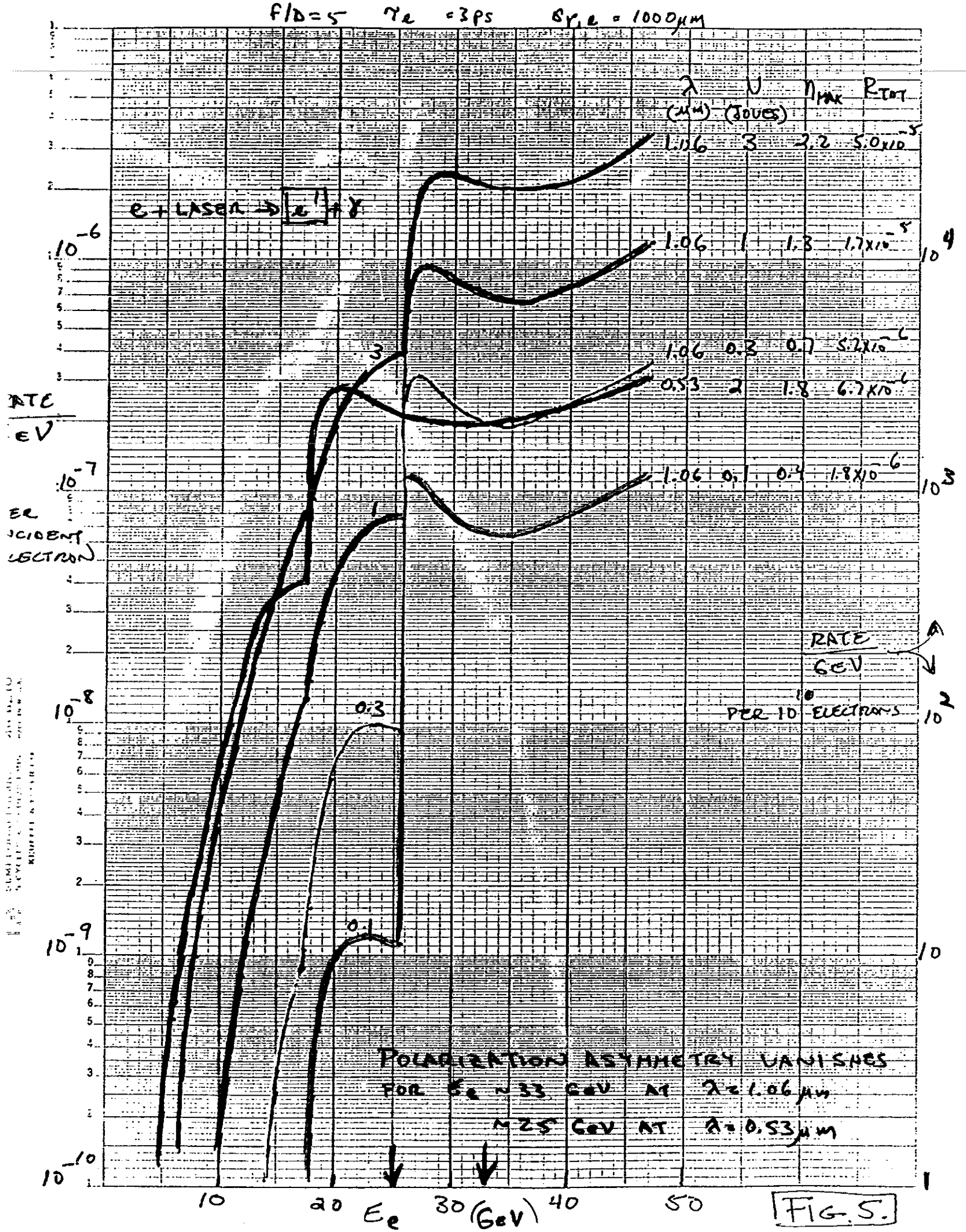
τLASER = 1ps
f/D = 5 τe = 3ps σr,e = 1000μm
λ (μm) U (JOULES) ηMAX RTOT
1.06 3 2.2 5.0×10^-5
1.06 1 1.3 1.7×10^-5
1.06 0.3 0.7 5.2×10^-6
0.53 2 1.8 6.7×10^-6
1.06 0.1 0.4 1.8×10^-6
e + LASER → [e'] + γ
RATE / eV
RATE / GeV
PER 10^10 ELECTRONS
POLARIZATION ASYMMETRY VANISHES
FOR Ee ~ 33 GeV AT λ = 1.06 μm
~25 GeV AT λ = 0.53 μm
Ee (GeV)
10 20 30 40 50

FIG. 5.

$\lambda = 1.06\,\mu m$ $\quad \eta = 2.2$ $\quad \tau_{laser} = 1\,ps$ $\quad \sigma_{r,laser} = 2.4\,\mu m$ $\quad \gamma = 1.0$ AT $E = 50G$

$U = 3$ Joules $\quad f/\# = 5$ $\quad \tau_e = 3\,ps$ $\quad \sigma_{r,e} = 1000\,\mu m$

MODEL DATE

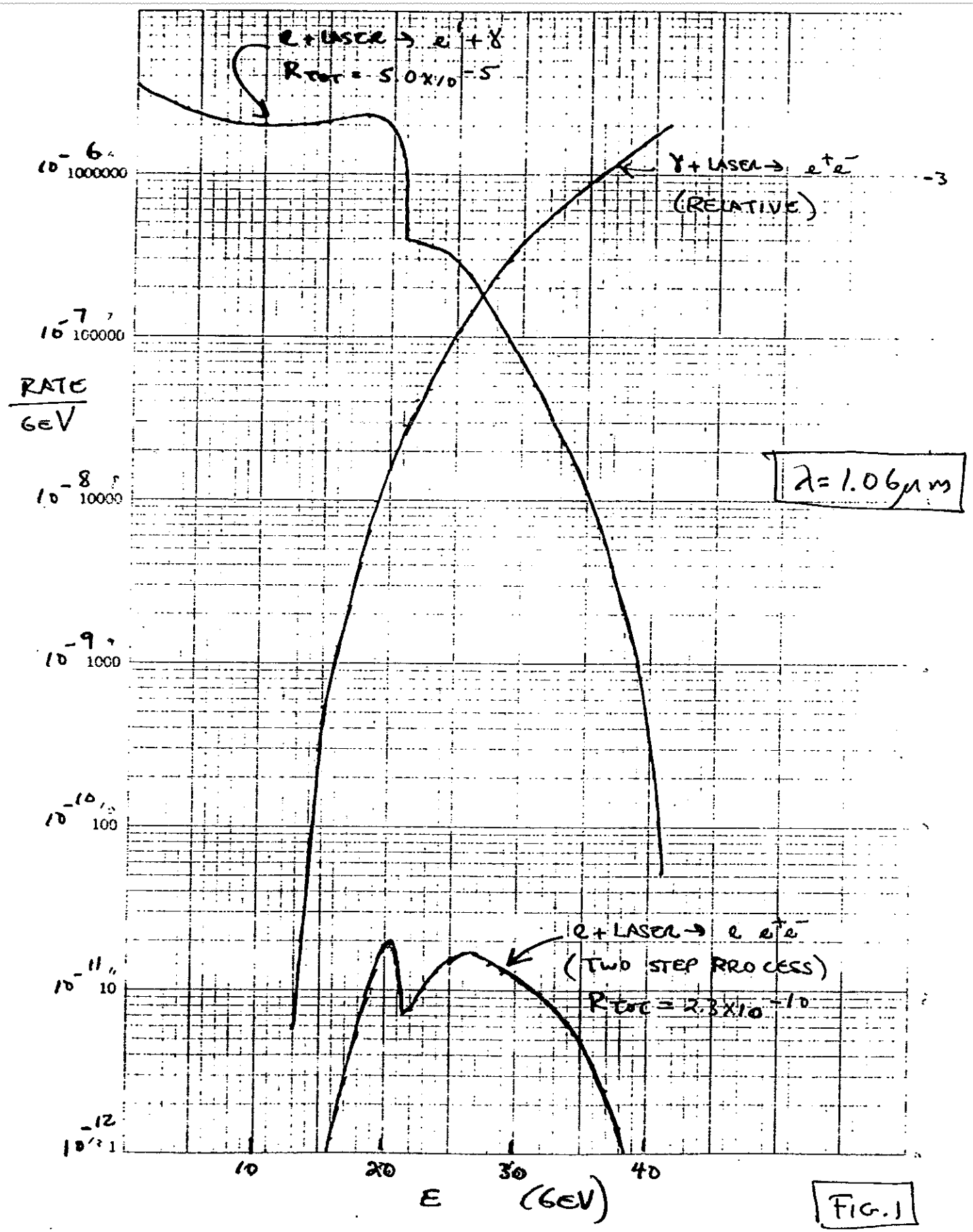


FIG. 1

$\lambda = 0.53\,\mu m$  $N = 1.8$  $\tau_{LASER} = 1\,ps$  $\sigma_{V,LASER} = 1.2\,\mu m$  $\gamma = 1.6$ KT $E = 50\,GeV$

$U = 2$ Joules  $f/D = 5$  $\tau_e < 3\,ps$  $\sigma_{V,e} = 1000\,\mu m$

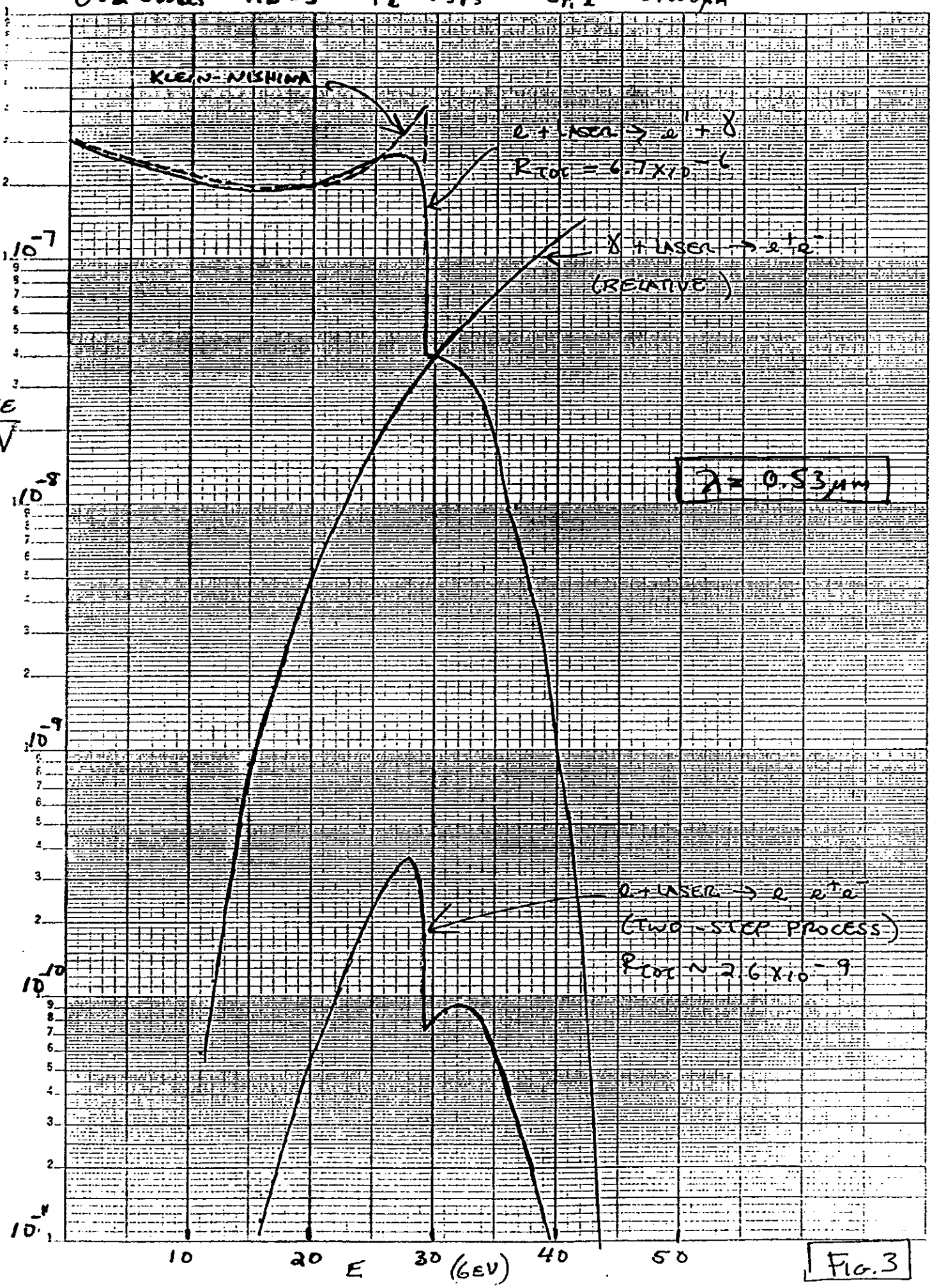


Fig. 3

1249>

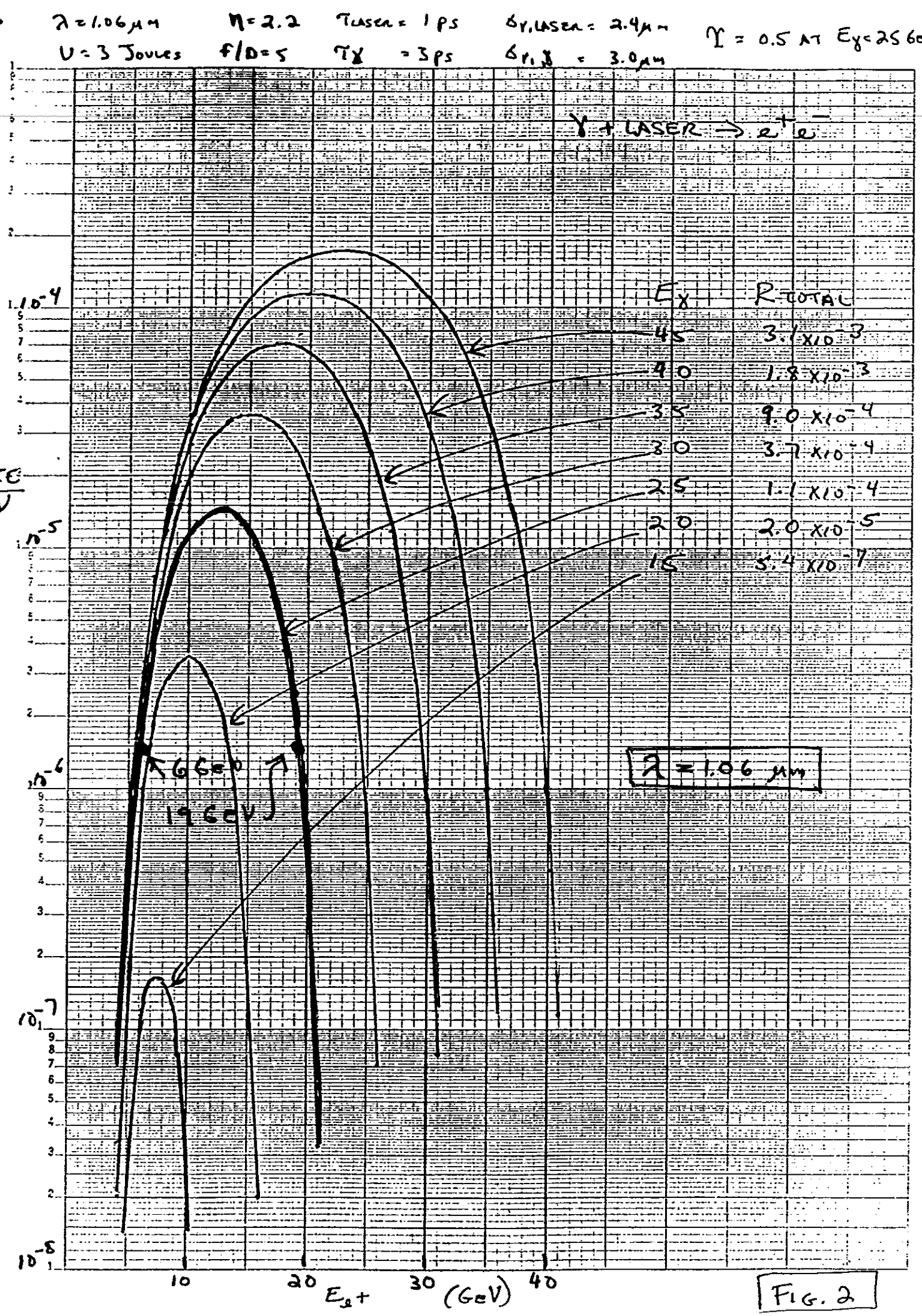
λ = 1.06 μm
η = 2.2
τLASER = 1 ps
σy,LASER = 2.4 μm
U = 3 Joules
f/D = 5
τγ = 3 ps
σy,γ = 3.0 μm
ϒ = 0.5 AT Eγ = 25 GeV
γ + LASER → e+e−
Eγ
R TOTAL
45 3.1 X10-3
40 1.8 X10-3
35 9.0 X10-4
30 3.7 X10-4
25 1.1 X10-4
20 2.0 X10-5
15 3.4 X10-7
RATE / GeV
10-4
10-5
10-6
10-7
10-8
6 GeV
12 GeV
λ = 1.06 μm
10
20
30
40
Ee+ (GeV)

FIG. 2

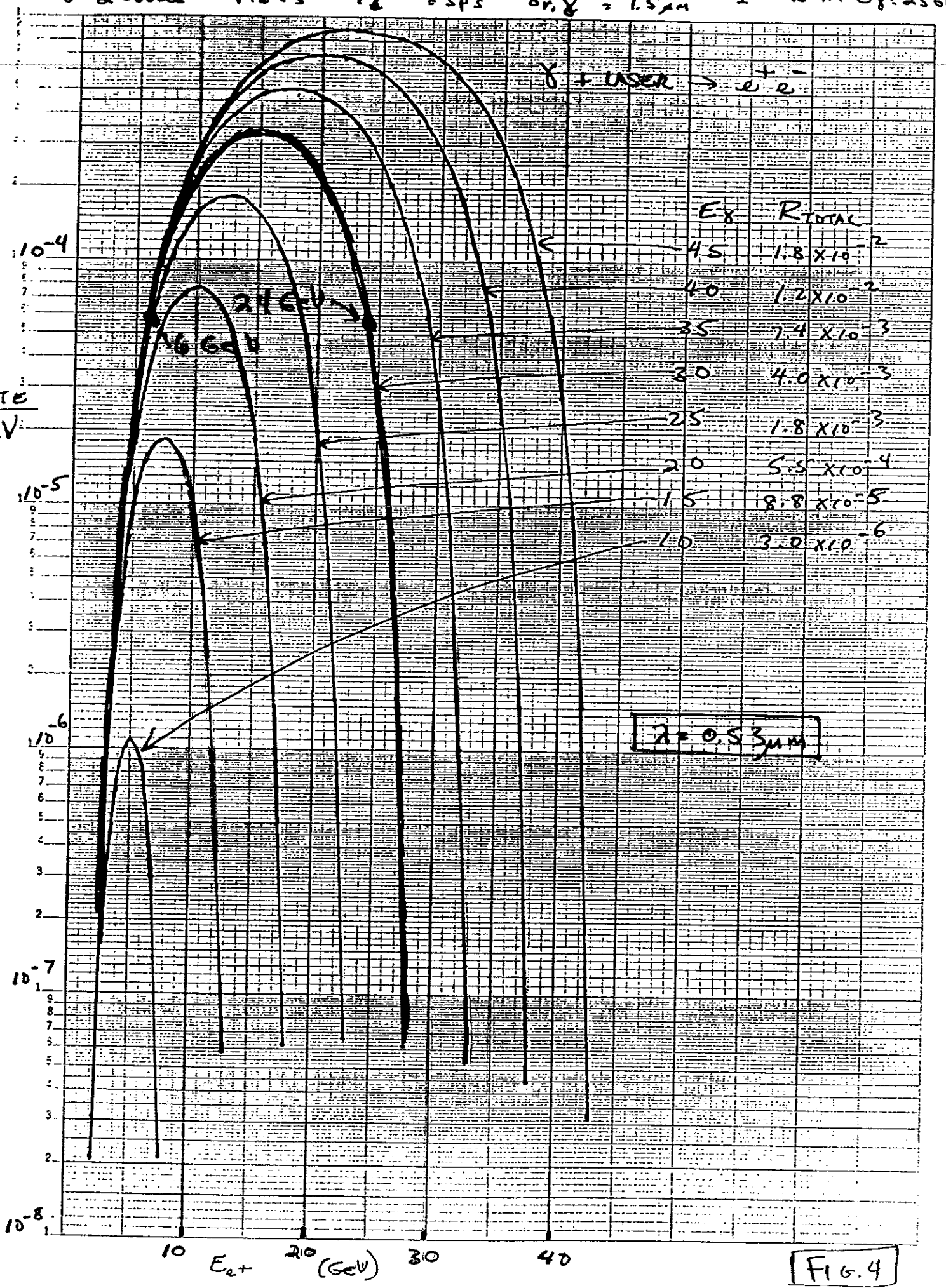
λ = 0.53 μm
U = 2 JOULES
η = 1.8
f/D = 5
τ LASER = 1 ps
τ γ = 3 ps
σr LASER = 1.2 μm
σr, γ = 1.5 μm
Υ = 0.8 AT Eγ = 25 GeV
γ + LASER → e+ e−
Eγ
R TOTAL
45
1.8 X10−2
40
1.2 X10−2
35
7.4 X10−3
30
4.0 X10−3
25
1.8 X10−3
20
5.5 X10−4
15
8.8 X10−5
10
3.0 X10−6
21 GeV
16 GeV
λ = 0.53 μm
RATE / GeV
10−4
10−5
10−6
10−7
10−8
10
20
30
40
Ee+ (GeV)

FIG. 4